Quasi-continuous wave Raman lasers at 990 and 976 nm based on a three-level Nd:YLF laser

Dimitri Geskus,[1] Jonas Jakutis Neto,[1] Saara-Maarit Reijn,[1] Helen M. Pask,[2] and Niklaus U. Wetter[1,*]

[1]*Centro de Lasers e Aplicações, IPEN/SP, Av. Prof. Lineu Preses, 2242 São Paulo, SP, Brazil*

[2]*MQ Photonics, Department of Physics and Astronomy, Macquarie University, NSW 2109, Australia*

**Corresponding author: nuwetter@ipen.br*

Received January 28, 2014; revised April 4, 2014; accepted April 13, 2014;
posted April 14, 2014 (Doc. ID 205482); published May 13, 2014

An intracavity Raman laser based on laser transition in Nd:YLF is reported. Quasi-continuous wave Stokes output power was observed at 990 and 976 nm, and up to 0.88 W of peak output power was obtained at 990 nm.

OCIS codes: (140.3530) Lasers, neodymium; (140.3550) Lasers, Raman; (190.2620) Harmonic generation and mixing.
http://dx.doi.org/10.1364/OL.39.002982

Crystalline Raman lasers offer a practical and efficient means of frequency conversion and generate output in a variety of temporal formats that include both pulsed and continuous-wave (cw) regimes. Intracavity Raman lasers can be physically very simple, and they are highly compatible with well-developed Nd lasers; additionally, many Raman-active media have been used successfully, most notably vanadates and tungstates [1,2]. The output wavelengths that can be achieved in the near-infrared range depend on the fundamental laser wavelength and the Raman shift of the Raman-active media. Output in the visible range can also be obtained by incorporating intracavity sum frequency mixing of the fundamental and/or Stokes wavelengths. The vast majority of intracavity Raman lasers have utilized the 1 μm Nd transition in various host crystals, which leads to multi-watt operation in the near-infrared range with efficiencies up to 13% [3] and wavelength-versatile operation in the red-yellow-lime spectral region [4,5].

To the best of our knowledge, there has been no report of intracavity Raman lasers based on the three-level transition of Nd gain media around 0.9 μm. Lasers based on this transition are challenging to design, owing to reabsorption losses at the fundamental frequency. Yet the generation of Stokes output below 1000 nm would be of tremendous interest as a stepping stone to obtaining laser emission in the blue region via second harmonic generation (SHG) and sum-frequency generation (SFG). A solid-state laser operating at 488 nm is just one example of a laser source that would attract strong interest. Other techniques such as frequency doubled semiconductor lasers [6] do have certain advantages, but they do not permit generation of a broad array of emission lines (50 nm) in the blue–green spectra. In this paper we present, to the best of our knowledge, the first intracavity Raman laser based on the fundamental wavelength of a three-level $Nd:YLiF_4$ (Nd:YLF) laser. Nd:YLF lasers are known to offer excellent beam quality, weak thermal lensing, and high efficiency for low duty cycle operation [7,8]. We have previously investigated a Nd:YLF/KGW (potassium gadolinium tungstate) Raman laser based on the 1053 nm fundamental, which gave rise to watt-level powers at six different near-infrared and visible output wavelengths [5].

In this paper, quasi-cw (q-cw) laser performance at 908 nm was analyzed using three different Nd:YLF crystal lengths and two different excitation wavelengths: 797 and 806 nm. A maximum output power of 7.7 W at 908 nm was found using a 6 mm long Nd:YLF crystal, which was excited at 797 nm. A KGW crystal was introduced into the cavity, and this resulted in Raman laser oscillation at 990 nm with a peak output power of 0.88 W; additionally, laser oscillation at 976 nm was observed. While cw Raman laser operation has been observed, extraction of significant output power has not been attempted to reduce the risk of damaging the optics, which would jeopardize future blue laser experiments.

In order to reach the threshold for cw or q-cw stimulated Raman scattering (SRS) high fundamental power densities are required inside the Raman crystal. Accordingly, the performance at 908 nm of a Nd:YLF laser was investigated in order to identify the most suitable cavity design. Nd(0.7%):YLF crystals that were 3 mm in diameter, and with lengths of 3, 6, and 9 mm, were mounted into water cooled copper mounts using indium foil and evaluated. The end faces of the crystals were coated with broadband anti-reflection (AR) coatings ($R < 0.2\%$ at 908 nm, $R < 0.1\%$ at 990 nm). The laser cavity consisted of a concave pump mirror (radius of curvature or ROC = 100 mm) with a high reflectivity (HR) ($R > 99.98\%$) for the laser wavelengths (908–990 nm) and high transmission ($T > 90\%$) at the pump wavelengths (797–806 nm), and a plane output coupler with a transmission of 1.14%, see Fig. 1.

The laser was pumped by a fiber-coupled diode laser whose output wavelength could be temperature tuned from 797 to 806 nm. The output from the fiber was focused to a spot radius of ~100 μm into the Nd:YLF

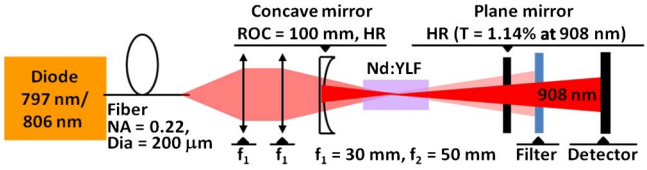

Fig. 1. Schematic representation of the setup used to characterize fundamental laser emissions.

crystal. The cavity length was approximately 45 mm, which provided a beam radius of the fundamental laser mode that ranged from 120 to 160 μm along the length of the cavity. The π-polarized fundamental laser performance at 908 nm was evaluated using two pump wavelengths, 797 and 806 nm, that matched the absorption peaks in Nd:YLF. For operation at 806 nm, the diode laser was operated in cw mode at a temperature of 18°C–32°C, depending on the diode current, and it had a spectral linewidth (FWHM) of 2 nm. The duty cycle was set to 2.9% using a mechanical chopper at a frequency of 50 Hz with a corresponding on-time of 580 μs. To reach the emission wavelength of 797 nm, the laser diode was operated at 10°C in pulsed mode with a low duty cycle of 1.7% at a frequency of 25 Hz with a corresponding on-time of 691 μs. Broadening of the emission linewidth to ~4 nm was observed, which was caused by a non-compensated thermal offset of the two individual laser diode bars in the diode laser source. The emission spectrum shifted to longer wavelengths at larger pump powers above 45 W, which resulted in decreased pump absorption and caused a "rollover" in some of the laser experiments.

The transmission of the pump mirror and the focusing optics was measured to be 87% and the absorption of the 6 mm long crystal was measured to be 71% at 797 nm, from which we deduced an absorption of 46% and 84% for the 3 and 9 mm long crystals, respectively. At 806 nm, a lower pump absorption of 64% for the 6 mm long crystal was measured, which gave an absorption of 40% and 78% for the 3 and 9 mm long crystals, respectively.

Laser performance at 908 nm was investigated with no KGW crystal present inside the cavity. At the non-pumped side of the 9 mm long crystal, visible fluorescence was observed under lasing conditions, which was attributed to excitation of the neodymium ions upon initiation of the intracavity laser field; this was indicative of excessive reabsorption and thus limits the laser efficiency and output power. Such strong fluorescent behavior was not observed in the 3 and 6 mm crystals, which is indicative of pump saturation and low reabsorption losses throughout the crystal. The q-cw laser performance at 908 nm is presented as a function of the absorbed pump power in Fig. 2. Note that the powers reported are the peak values that were obtained during the pump "on-time." The lowest threshold of only 1.5 W absorbed pump power was obtained using the 3 mm long crystal because this crystal had the lowest reabsorption losses; hence, it provided the highest optical to optical (diode to fundamental) efficiency of 30%. However, the maximum output power was limited because of the reduced pump absorption. The maximum laser output power of 7.7 W for a launched pump power of 53 W (33 W absorbed power) was achieved using the 6 mm long crystal under 797 nm pumping.

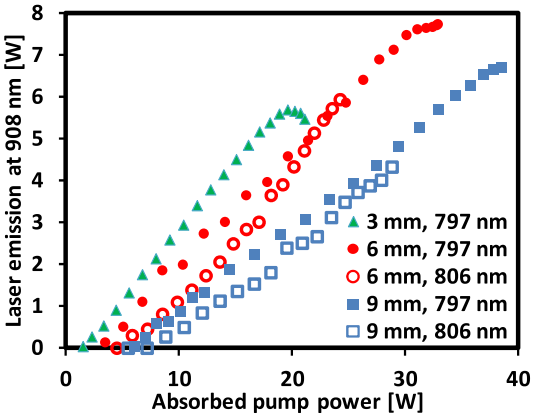

Fig. 2. Quasi-cw laser performance at 908 nm for three crystal lengths (3, 6, and 9 mm) at different pump wavelengths (797 and 806 nm).

The corresponding overall efficiency with respect to the absorbed pump power was 23%. Accordingly, the combination of pumping a 6 mm long Nd:YLF laser crystal at 797 nm was selected for the investigation of Raman laser action.

The KGW crystals that were 5, 10, and 25 mm in length were consecutively introduced inside the cavity in order to initiate SRS. The orientation of the KGW crystals was $E\|N_m$ to access the 901 cm^{-1} Stokes shift. The crystals were mounted into a copper mount using indium foil. The best performance was obtained using two concave mirrors with a ROC = 50 mm; this resulted in a beam waist near the center of the cavity of 62 μm for a cavity length of 102 mm. The laser crystal was placed at approximately 25 mm from the pump entrance mirror to achieve good mode-matching between the pump beam radius of 100 μm and the laser mode radius of 130 μm. The pump input mirror had HR ($R > 99.98\%$) at 908 nm and 990 nm, and the outcoupling mirror had HR ($R > 99.98\%$) at 908 nm and a transmission of $T_s = 0.28\%$ at 990 nm, see Fig. 3. The best Raman laser performance at 990 nm was obtained using the 10 mm long KGW crystal. Laser emission commenced at an absorbed pump power of 5.4 W, and a maximum output power of 0.88 W was achieved. About 0.5 W of output power was observed using the 5 mm long KGW crystal. However, after only a few seconds of operation the coating of the Nd:YLF crystal became damaged. We believe that the reduced conversion efficiency by the shorter KGW crystal resulted in a larger intracavity power of the fundamental, which caused the defect.

Further damage was avoided by moving the position of the Nd:YLF crystal closer to the mirror, thereby having a larger laser mode diameter to prevent further damage. This safety measure obviously reduced the laser efficiency, as can be seen in Fig. 4. A blue fluorescence, which was attributed to crystal impurities [9], was observed inside the KGW crystal upon Raman laser oscillation.

The 1st Stokes laser emission at 976 nm was obtained when the KGW was oriented having $E\|N_g$ to utilize the 768 cm^{-1} Stokes shift. While the threshold was similar to the experiment at 990 nm, the output power was very

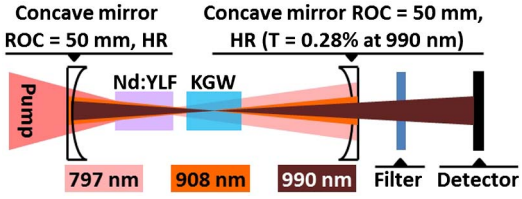

Fig. 3. Schematic representation of the setup used to measure Raman laser operation using a KGW crystal.

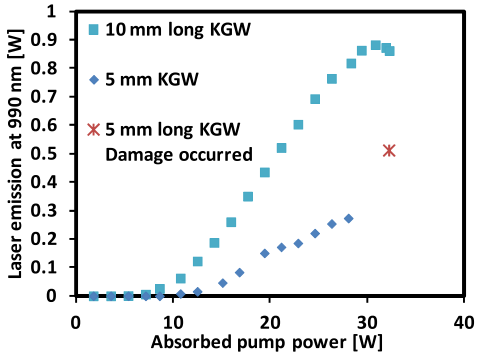

Fig. 4. Laser performance of the Raman laser at 990 nm for KGW crystal lengths of 5 and 10 mm.

low due to low output transmission of the mirror ($T < 0.01\%$). Based on Ref. [5], we anticipate that the performance at 976 nm could be similar to that at 990 nm if a higher output coupling was used (no suitable mirror was available to investigate this further). The spectra of the two Raman laser emission lines, which are shown in Fig. 5, were measured using an Ocean Optics HR2000 spectrophotometer with a resolution of 0.24 nm. Both emission lines had a fairly broad emission width of ~2 nm (FWHM).

The spectrum of the fundamental was observed with and without the KGW Raman crystal in the resonator, and as shown in Fig. 6, the SRS process was associated with a doubling of the linewidth. This broadening effect can be credited to the SRS process presenting loss to the center of the fundamental line [10]. The broad emission linewidth (36 cm^{-1}) [11] for Nd:YLF relative to the KGW Raman gain bandwidth (5.4 cm^{-1}) [12] makes the system highly susceptible to such broadening. The M^2 measurements were performed by focusing the beam of the laser emission onto a CCD camera using a biconvex lens ($f = 125$ mm) at a distance of 28 cm from the cavity center. The camera was translated through the focal plane, while we measured the beam waist using the second moment beam analysis in the x and y directions. M^2 values between 1 and 1.1 were found for both the Stokes and fundamental beams. The analysis for the Stokes beam is shown in Fig. 7.

A numerical model for intracavity Raman lasers [13] was adapted to predict the laser behavior of an intracavity Raman laser having a quasi-three-level fundamental laser:

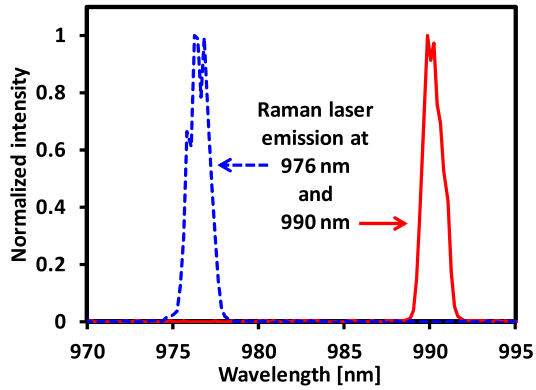

Fig. 5. Observed normalized Raman laser spectra.

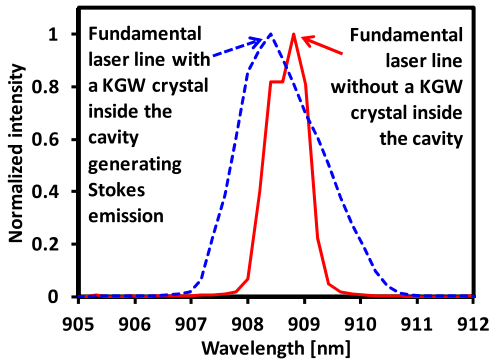

Fig. 6. Spectral broadening of the fundamental laser emission by intracavity generated 1st Stokes.

$$\frac{P_f}{dt} = \frac{c\sigma_G N^* P_f l_l}{l} - \frac{cP_f P_s G_r l_r}{lA_r \frac{\lambda_f}{\lambda_s}} - \frac{cP_f(T_f + L_f)}{2l} - \frac{c\sigma_R(N^d - N^*)P_f l_l}{l},$$

$$\frac{P_s}{dt} = \frac{cP_f P_s G_r l_r}{lA_r} - \frac{cP_s(T_s + L_s)}{2l},$$

$$\frac{N^*}{dt} = \frac{P_p \lambda_p}{hcA_l l_l} - \frac{2\lambda_f \sigma_G N^* P_f}{hcA_l} - \frac{N^*}{\tau_l} + \frac{2\lambda_f \sigma_R (N^d - N^*)P_f}{hcA_l} - N^{*2} W_{\mathrm{ETU}}.$$

To incorporate the thermal population of the lower laser level in the model, the on-axis Nd:YLF crystal temperature was simulated using a MATLAB code based on Ref. [14]. The simulated temperature rise at the optical axis was 12°C at the end of the pump pulse corresponding to an effective reabsorption cross section according to the McCumber theory [15] of $\sigma_R = 0.093 \cdot 10^{-24}$ m^2 based on the emission cross section $\sigma_G = 1.25 \cdot 10^{-24}$ m^2 at 908 nm [11]. The model predicts a high population inversion of about 10–15%, therefore it was essential to add energy transfer upconversion, $W_{\mathrm{ETU}} = 1.7 \cdot 10^{-16}$ cm^3 [16], to the model, which reduced the calculated laser efficiency by 5%.

The optical to optical (diode to Stokes) efficiencies predicted by this model are presented in Fig. 8, and these were obtained using the input data presented in Table 1. The round trip loss was used as a fitting parameter to give

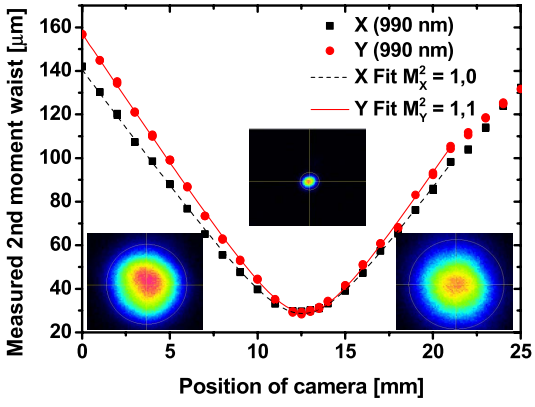

Fig. 7. M^2 measurement of Raman laser beam with beam profiles at far-field, in focus, and far-field.

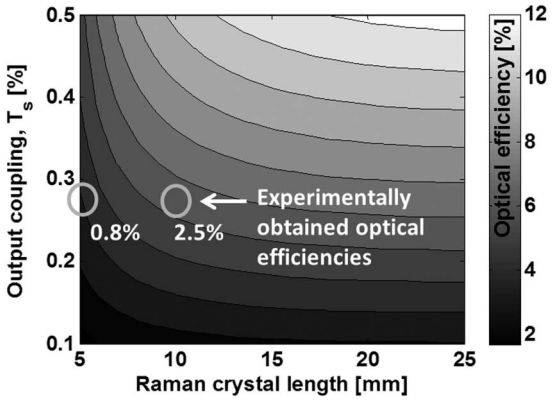

Fig. 8. Modeled efficiency of the Raman laser as a function of the Raman crystal length (l_r) and output coupling transmission for Stokes (T_s) at an absorbed pump power (P_p) of 33 W.

Table 1. Input Parameters for the Rate Equation Model

T_s	0.28%	Output coupling for Stokes
T_f	0.02%	Output coupling for fundamental
A_l	$31\ \mu m \cdot 10^3\ \mu m$	Spot area in laser crystal ($r = 100\ \mu m$)
A_r	$15\ \mu m \cdot 10^3\ \mu m$	Spot area in Raman crystal ($r = 70\ \mu m$)
l_l	6 mm	Length of laser crystal
τ_l	485 μs	Upper laser level lifetime
G_r	$4.4 \cdot 10^{-11}$ m/W	Stimulated Raman gain coefficient
c	$3 \cdot 10^8$ m/s	Speed of light through vacuum
h	$6.62 \cdot 10^{-34}$ Js	Planck's constant
N^d	$0.98 \cdot 10^{26}\ m^{-3}$	Doping concentration
l	0.1147 m	Optical cavity length
λ_p, λ_f, λ_s, wavelength of pump, fundamental, and Stokes		

reasonable agreement between the model predictions and experiment. A fairly large round trip loss of 2% for both fundamental (L_f) and Raman (L_s) lasers was required to reach agreement. However, the simple character of the model makes it more useful for predicting trends than predicting exact values for efficiency. The model predicts more than a doubling of the efficiency if these losses could be halved. As shown in Fig. 8, an improved laser performance is predicted for higher output coupling; this will be tested in the near future by using intracavity SHG to convert the Stokes emission to blue. In addition, an improved efficiency for longer Raman crystals is predicted. However, introduction of a 25 mm long Raman crystal into the cavity remarkably resulted in generation of short 1st Stokes pulses with durations of ~100 ns with a pulse separation of about 1.3 μs. We speculate that this is some kind of self Q-switching behavior, the dynamics of which will be investigated in the near future.

We have demonstrated, to the best of our knowledge, the first intracavity Raman laser that is based upon a quasi-three-level Nd laser. Despite strong reabsorption losses at the 908 nm laser fundamental, intracavity Raman laser generation is viable. However, when compared to four-level operation in a very similar setup of Nd:YLF-KGW [5], the three-level laser generated 1st Stokes signal was approximately three times weaker at 21 W of absorbed pump power. The experimentally obtained data was analyzed using a simple steady-state rate equation model. The model indicates considerable intracavity loss of about 2% in our laser cavity. The model predicts improved laser output power for higher output coupling and using longer Raman crystals. Experiments suggest that too long Raman crystals provide a too strong coupling of the fundamental laser to the Stokes laser field, which results in pulsed Stokes. Using this Nd:YLF-KGW laser scheme, we demonstrated a maximum output power of 7.7 W at 908 nm and 0.88 W at 990 nm. Similar Stokes output powers are expected at 976 nm using optimized outcoupling efficiencies.

This research demonstrates the feasibility of cw Raman lasers based on fundamental emission from three-level neodymium lasers. Given that the newly obtained wavelengths in the 9xx nm region can easily be converted to the blue wavelength region using traditional SFG and SHG, this research should spark a series of developments in the area of high intensity blue lasers at new, blue wavelengths.

Acknowledgment: this research project was financially supported by CNPq project no. 401580/2012.

References

1. T. T. Basiev and R. C. Powell, Opt. Mater. **11**, 301 (1999).
2. H. M. Pask, Prog. Quantum Electron. **27**, 3 (2003).
3. L. Fan, Y. X. Fan, Y. Q. Li, H. J. Zhang, Q. Wang, J. Wang, and H. T. Wang, Opt. Lett. **34**, 1687 (2009).
4. A. J. Lee, H. M. Pask, J. A. Piper, H. Zhang, and J. Wang, Opt. Express **18**, 5984 (2010).
5. J. Jakutis-Neto, J. Lin, N. U. Wetter, and H. Pask, Opt. Express **20**, 9841 (2012).
6. L. Fan, T.-C. Hsu, M. Fallahi, J. T. Murray, R. Bedford, Y. Kaneda, J. Hader, A. R. Zakharian, J. V. Moloney, S. W. Koch, and W. Stolz, Appl. Phys. Lett. **88**, 251117 (2006).
7. N. U. Wetter, E. C. Sousa, I. M. Ranieri, and S. L. Baldochi, Opt. Lett. **34**, 292 (2009).
8. N. U. Wetter and A. M. Deana, Laser Phys. Lett. **10**, 035807 (2013).
9. J. Jakutis-Neto, C. Artlett, A. J. Lee, J. Lin, D. J. Spence, J. A. Piper, N. U. Wetter, and H. M. Pask, Opt. Mater. Express **4**, 889 (2014).
10. G. M. Bonner, J. Lin, A. J. Kemp, J. Wang, H. Zhang, D. J. Spence, and H. M. Pask, Opt. Express **22**, 7492 (2014).
11. C. Czeranowsky, "Resonatorinterne frequenzverdopplung von diodengepumpten neodym-lasern mit hohen ausgangsleistungen im blauen spektralbereich," Ph.D. thesis (University of Hamburg, 2002).
12. T. T. Basiev, A. A. Sobol, P. G. Zverev, V. V. Osiko, and R. C. Powell, Appl. Opt. **38**, 594 (1999).
13. D. J. Spence, P. Dekker, and H. M. Pask, IEEE J. Sel. Top. Quantum Electron. **13**, 756 (2007).
14. E. H. Bernhardi, A. Forbes, C. Bollig, and M. J. D. Esser, Opt. Express **16**, 11115 (2008).
15. D. E. McCumber, Phys. Rev. **136**, A954 (1964).
16. P. J. Hardman, W. A. Clarkson, G. J. Friel, M. Pollnau, and D. C. Hanna, IEEE J. Quantum Electron. **35**, 647 (1999).